

Supplementary Tables

Supplementary Table 1: Differentially expressed miRNAs between *F nucleatum*-treated and untreated cells.

miRNA	p-value	FDR	Log2 (FC)	Untreated				<i>F nucleatum</i> -treated			
				HCT116	HT29	LoVo	SW480	HCT116	HT29	LoVo	SW480
hsa-miR-4773	6.02E-05	6.14E-03	-10.98	5	12	10	49	0	0	0	0
hsa-let-7f-5p	1.03E-04	5.24E-03	2.67	1,103	1,243	1,012	1,599	8,825	8,608	5,168	8,872
hsa-let-7i-5p	2.94E-04	9.99E-03	3.65	102	257	113	140	2,466	2,096	1,022	2,103
hsa-miR-23a-3p	4.77E-04	1.22E-02	2.74	665	1,226	670	1,182	7,751	6,887	3,722	6,620
hsa-let-7a-5p	5.56E-04	1.13E-02	2.60	798	1,428	862	1,336	8,192	7,414	3,821	7,430
hsa-miR-6837-3p	5.90E-04	1.00E-02	-10.41	8	35	2	4	0	0	0	0
hsa-miR-6837-5p	7.34E-04	1.07E-02	-12.27	6	28	143	6	0	0	0	0
hsa-miR-23b-3p	7.40E-04	9.44E-03	2.79	579	1,205	616	935	6,968	6,551	3,040	6,457
hsa-miR-21-5p	7.90E-04	8.95E-03	2.12	1,495	1,696	1,514	2,085	8,978	8,173	4,804	7,552

miRNA	p-value	FDR	Log2 (FC)	Untreated				<i>F. nucleatum</i> -treated			
				HCT116	HT29	LoVo	SW480	HCT116	HT29	LoVo	SW480
				hsa-miR-24-2-5p	8.86E-04	9.04E-03	3.17	9	12	10	19
hsa-miR-27b-3p	1.53E-03	1.42E-02	3.29	64	162	78	96	1,261	1,199	363	1,086
hsa-miR-31-3p	1.79E-03	1.52E-02	5.49	2	8	1	7	362	191	48	190
hsa-miR-24-3p	2.10E-03	1.65E-02	2.31	1,554	2,844	1,145	2,560	11,217	11,249	7,577	10,002
hsa-let-7b-5p	2.36E-03	1.72E-02	3.70	76	279	69	86	2,386	2,593	733	924
hsa-miR-27a-3p	3.19E-03	2.17E-02	2.61	131	374	145	207	1,529	1,827	591	1,285
hsa-miR-34a-5p	3.23E-03	2.06E-02	4.50	4	6	4	4	197	84	50	50
hsa-miR-30a-5p	3.79E-03	2.27E-02	1.11	1,957	1,575	2,233	1,388	4,709	3,846	2,831	4,025
hsa-miR-4789-3p	3.91E-03	2.21E-02	-9.20	63	7	115	2	0	0	0	0
hsa-miR-99a-5p	4.04E-03	2.17E-02	1.88	248	236	245	125	799	1,121	438	788
hsa-miR-4306	4.55E-03	2.32E-02	-2.17	285	765	394	474	95	97	178	57

miRNA	p-value	FDR	Log2 (FC)	Untreated				<i>F. nucleatum</i> -treated			
				HCT116	HT29	LoVo	SW480	HCT116	HT29	LoVo	SW480
				hsa-miR-221-3p	4.99E-03	2.42E-02	4.81	6	80	12	6
hsa-miR-22-3p	5.25E-03	2.44E-02	1.82	231	437	240	329	1,462	943	577	1,373
hsa-miR-7977	5.44E-03	2.41E-02	-1.01	982	1,333	835	779	393	471	596	493
hsa-miR-19a-3p	5.56E-03	2.36E-02	-2.42	772	1,939	1,073	623	95	242	317	171
hsa-miR-125b-5p	5.78E-03	2.36E-02	2.80	179	127	117	152	1,588	671	554	1,203
hsa-miR-378f	6.20E-03	2.43E-02	-1.87	584	371	385	259	102	64	196	75
hsa-miR-22-5p	6.63E-03	2.51E-02	1.80	9	21	11	17	86	42	34	44
hsa-miR-181a-2-3p	6.64E-03	2.42E-02	1.78	6	5	12	4	37	21	18	17
hsa-miR-98-5p	6.81E-03	2.40E-02	3.39	36	163	70	32	597	1,554	245	755
hsa-miR-31-5p	6.95E-03	2.36E-02	5.67	3	114	15	6	3,289	963	465	2,294
hsa-miR-23c	7.57E-03	2.49E-02	3.38	68	234	82	84	1,238	1,654	265	1,718

miRNA	p-value	FDR	Log2 (FC)	Untreated				<i>F. nucleatum</i> -treated			
				HCT116	HT29	LoVo	SW480	HCT116	HT29	LoVo	SW480
				hsa-miR-4324	7.72E-03	2.46E-02	2.38	125	186	114	72
hsa-miR-196a-5p	7.92E-03	2.45E-02	2.40	98	37	95	25	490	338	169	338
hsa-miR-100-5p	8.31E-03	2.49E-02	3.09	100	229	168	52	1,719	1,309	319	1,326
hsa-miR-125a-5p	8.68E-03	2.53E-02	0.93	398	262	336	238	678	500	536	635
hsa-miR-320a	9.25E-03	2.62E-02	0.60	414	305	343	434	668	558	556	494
hsa-miR-4454	1.02E-02	2.82E-02	-1.30	1,790	2,243	1,283	1,166	749	383	747	751
hsa-miR-4488	1.04E-02	2.79E-02	0.93	106	112	101	131	270	186	157	245
hsa-miR-1244	1.13E-02	2.96E-02	-0.93	83	55	88	74	46	27	38	47
hsa-miR-342-3p	1.29E-02	3.30E-02	-1.15	424	276	402	379	169	133	250	117
hsa-miR-331-3p	1.31E-02	3.27E-02	1.15	27	25	25	45	97	51	50	71
hsa-miR-130a-3p	1.36E-02	3.31E-02	2.29	38	205	107	84	809	465	299	559

miRNA	p-value	FDR	Log2 (FC)	Untreated				<i>F. nucleatum</i> -treated			
				HCT116	HT29	LoVo	SW480	HCT116	HT29	LoVo	SW480
				hsa-miR-148b-3p	1.38E-02	3.26E-02	1.27	543	494	434	577
hsa-miR-378e	1.39E-02	3.22E-02	-1.44	1,499	1,094	1,638	1,121	386	364	904	321
hsa-miR-5100	1.42E-02	3.21E-02	-1.38	104	75	63	85	41	41	26	17
hsa-miR-142-3p	1.50E-02	3.33E-02	-4.27	450	864	821	176	2	15	95	8
hsa-miR-4423-3p	1.61E-02	3.50E-02	-3.37	387	1,109	673	131	13	23	118	68
hsa-miR-146a-5p	1.64E-02	3.48E-02	-2.21	35	15	37	34	5	5	14	2
hsa-miR-185-5p	1.64E-02	3.41E-02	-1.74	470	916	423	877	169	97	403	133
hsa-miR-20a-3p	1.65E-02	3.36E-02	-2.39	198	519	207	334	31	38	148	23
hsa-miR-222-3p	1.66E-02	3.32E-02	4.82	5	84	13	2	1,078	809	288	761
hsa-miR-320b	1.71E-02	3.36E-02	0.55	298	217	272	281	483	351	394	335
hsa-miR-378i	1.76E-02	3.39E-02	-1.76	777	493	669	367	166	88	325	103

miRNA	p-value	FDR	Log2 (FC)	Untreated				<i>F. nucleatum</i> -treated			
				HCT116	HT29	LoVo	SW480	HCT116	HT29	LoVo	SW480
				hsa-miR-29a-3p	1.84E-02	3.48E-02	2.29	175	212	228	258
hsa-miR-193a-3p	1.85E-02	3.43E-02	2.84	58	62	47	18	329	346	72	583
hsa-miR-6512-3p	1.87E-02	3.41E-02	-5.99	66	45	2	19	0	2	0	0
hsa-miR-6089	1.88E-02	3.37E-02	0.68	474	313	497	346	736	631	567	673
hsa-miR-6803-5p	1.96E-02	3.45E-02	0.52	69	87	103	83	117	149	107	117
hsa-miR-3665	2.00E-02	3.45E-02	0.76	150	131	147	144	253	187	217	310
hsa-miR-148a-3p	2.06E-02	3.50E-02	2.02	65	39	62	81	338	219	90	355
hsa-miR-6793-5p	2.16E-02	3.62E-02	-5.36	5	2	55	5	0	0	2	0
hsa-let-7c-5p	2.26E-02	3.71E-02	3.22	45	978	367	259	3,917	4,892	1,320	5,223
hsa-miR-320c	2.26E-02	3.66E-02	0.64	305	201	236	274	488	365	426	306
hsa-miR-144-3p	2.49E-02	3.96E-02	-3.51	60	102	162	32	1	8	22	1

miRNA	p-value	FDR	Log2 (FC)	Untreated				<i>F. nucleatum</i> -treated			
				HCT116	HT29	LoVo	SW480	HCT116	HT29	LoVo	SW480
				hsa-miR-548w	2.64E-02	4.15E-02	-1.94	48	35	52	21
hsa-miR-193b-3p	2.65E-02	4.10E-02	3.07	115	69	66	69	1,150	428	160	940
hsa-miR-338-3p	2.99E-02	4.55E-02	4.31	0	5	0	0	13	76	10	3
hsa-miR-4793-5p	3.16E-02	4.74E-02	-4.28	2	30	7	45	0	4	0	0
hsa-miR-142-5p	3.18E-02	4.71E-02	-3.32	764	1,738	1,328	717	7	39	391	19
hsa-miR-19b-3p	3.22E-02	4.69E-02	-1.47	2,927	4,032	2,896	3,742	697	1,095	2,408	708
hsa-miR-340-5p	3.32E-02	4.78E-02	-1.14	165	146	211	123	49	102	101	40
hsa-miR-4443	3.34E-02	4.74E-02	-1.29	2,243	2,794	2,149	3,257	697	1,020	1,893	666
hsa-miR-17-3p	3.41E-02	4.77E-02	-2.09	165	184	132	193	27	11	103	18
hsa-miR-486-5p	3.43E-02	4.73E-02	-2.64	454	500	272	625	12	20	245	20
hsa-miR-126-3p	3.47E-02	4.72E-02	-2.05	2,241	2,759	2,347	2,617	233	223	1,736	218

miRNA	p-value	FDR	Log2 (FC)	Untreated				<i>F. nucleatum</i> -treated			
				HCT116	HT29	LoVo	SW480	HCT116	HT29	LoVo	SW480
				hsa-miR-939-3p	3.61E-02	4.85E-02	-10.91	15	47	0	4
hsa-miR-126-5p	3.74E-02	4.95E-02	-3.24	4	47	43	14	5	2	3	1
hsa-miR-3180	3.77E-02	4.93E-02	-4.59	16	2	9	39	0	0	0	3
hsa-miR-106a-5p	3.79E-02	4.90E-02	-1.51	4,387	5,331	4,819	4,883	817	1,547	3,609	869
hsa-miR-4497	3.81E-02	4.86E-02	1.22	117	133	109	142	441	250	160	318
hsa-miR-30e-5p	3.87E-02	4.88E-02	0.67	1,408	1,547	1,283	2,210	1,999	3,452	2,281	2,503
hsa-miR-378j	3.90E-02	4.85E-02	-3.63	26	32	41	13	0	9	0	0
hsa-miR-130b-3p	3.94E-02	4.84E-02	-2.11	1,377	1,517	1,309	1,862	92	117	1,089	103
hsa-miR-450b-3p	3.96E-02	4.81E-02	-8.57	17	35	0	6	0	0	0	0
hsa-miR-548d-3p	4.06E-02	4.87E-02	-3.94	9	37	5	35	6	0	0	0
hsa-miR-4525	4.09E-02	4.86E-02	-10.23	2	1	0	38	0	0	0	0

miRNA	p-value	FDR	Log2 (FC)	Untreated				<i>F. nucleatum</i> -treated			
				HCT116	HT29	LoVo	SW480	HCT116	HT29	LoVo	SW480
				hsa-let-7e-5p	4.14E-02	4.85E-02	2.31	455	837	512	328
hsa-miR-18a-3p	4.17E-02	4.83E-02	-2.30	167	234	170	252	16	12	133	6
hsa-miR-195-5p	4.21E-02	4.82E-02	0.61	51	81	91	78	140	113	103	102
hsa-miR-1260b	4.24E-02	4.81E-02	-1.13	1,077	2,224	1,160	2,577	960	613	718	930
hsa-miR-17-5p	4.26E-02	4.78E-02	-1.45	4,476	5,366	4,986	5,012	832	1,558	3,933	923
hsa-miR-20a-5p	4.29E-02	4.76E-02	-1.50	4,091	6,054	5,248	5,909	909	1,732	3,992	914
hsa-miR-938	4.35E-02	4.77E-02	-10.95	15	51	0	1	0	0	0	0
hsa-miR-18a-5p	4.39E-02	4.76E-02	-1.93	1,278	1,015	1,185	1,238	99	113	941	82
hsa-miR-424-5p	4.41E-02	4.73E-02	2.48	62	175	103	54	720	365	120	999
hsa-miR-15a-5p	4.59E-02	4.88E-02	-0.60	574	519	624	368	341	352	315	367
hsa-miR-378g	4.65E-02	4.89E-02	-1.47	940	600	772	551	248	113	525	149

miRNA	p-value	FDR	Log2 (FC)	Untreated				<i>F. nucleatum</i> -treated			
				HCT116	HT29	LoVo	SW480	HCT116	HT29	LoVo	SW480
				hsa-miR-451a	4.66E-02	4.85E-02	-2.30	2,988	3,184	2,886	3,293
hsa-miR-4793-3p	4.75E-02	4.89E-02	-10.03	8	17	0	56	0	0	0	0
hsa-miR-3065-5p	4.83E-02	4.93E-02	2.44	0	3	3	6	33	13	8	12
hsa-miR-3138	4.88E-02	4.93E-02	-3.74	8	9	1	47	0	5	0	0
hsa-miR-18b-5p	4.90E-02	4.90E-02	-2.00	973	783	859	907	70	60	718	34
hsa-miR-548h-3p	5.02E-02	/	-4.15	37	33	31	24	0	6	1	0
hsa-miR-6838-3p	5.03E-02	/	-11.18	9	41	34	0	0	0	0	0
hsa-miR-223-3p	5.04E-02	/	-2.24	2,167	1,832	2,751	1,859	33	35	1,677	76
hsa-miR-320e	5.19E-02	/	0.55	254	195	210	270	423	350	353	235
hsa-miR-503-5p	5.28E-02	/	2.60	2	4	8	11	93	22	8	22
hsa-miR-20b-5p	5.37E-02	/	-1.80	927	3,639	1,170	812	177	1,093	297	311

miRNA	p-value	FDR	Log2 (FC)	Untreated				<i>F. nucleatum</i> -treated			
				HCT116	HT29	LoVo	SW480	HCT116	HT29	LoVo	SW480
				hsa-miR-937-5p	5.44E-02	/	-2.86	31	38	25	5
hsa-miR-29c-3p	5.68E-02	/	1.78	46	48	64	15	75	315	69	136
hsa-miR-196b-5p	5.85E-02	/	4.14	6	0	1	0	37	64	14	12
hsa-miR-338-5p	5.98E-02	/	4.37	0	4	0	1	14	67	17	1
hsa-miR-3196	6.00E-02	/	0.57	52	41	61	64	102	61	93	67
hsa-miR-4772-5p	6.08E-02	/	-2.35	6	16	34	33	0	18	0	0
hsa-miR-6085	6.09E-02	/	-0.55	65	56	55	37	34	41	28	42
hsa-miR-301b	6.19E-02	/	-1.77	270	121	261	205	20	25	191	14
hsa-miR-378c	6.23E-02	/	-1.41	545	298	415	304	160	57	294	76
hsa-miR-1275	6.27E-02	/	-0.93	238	420	235	397	102	215	259	104
hsa-miR-130b-5p	6.31E-02	/	-2.30	108	144	62	141	9	6	76	1

miRNA	p-value	FDR	Log2 (FC)	Untreated				<i>F. nucleatum</i> -treated			
				HCT116	HT29	LoVo	SW480	HCT116	HT29	LoVo	SW480
				hsa-miR-7160-5p	6.32E-02	/	-10.21	0	1	4	40
hsa-miR-3960	6.49E-02	/	0.34	269	226	283	336	322	328	418	340
hsa-miR-186-5p	6.49E-02	/	-0.61	787	877	880	918	450	550	849	422
hsa-miR-6506-5p	6.54E-02	/	3.44	5	0	0	1	10	6	34	11
hsa-miR-4778-5p	6.56E-02	/	-1.37	30	52	50	35	17	25	17	5
hsa-miR-30a-3p	6.73E-02	/	4.00	0	17	3	0	127	122	26	53
hsa-let-7g-3p	6.77E-02	/	-11.28	0	76	6	0	0	0	0	0
hsa-miR-574-5p	6.86E-02	/	1.30	37	33	9	39	116	80	41	54
hsa-miR-203a	7.02E-02	/	4.39	0	3	3	1	62	42	7	31
hsa-miR-574-3p	7.20E-02	/	1.45	32	67	37	40	203	123	41	113
hsa-miR-379-3p	7.25E-02	/	-2.10	79	2	101	137	0	0	74	0

miRNA	p-value	FDR	Log2 (FC)	Untreated				<i>F. nucleatum</i> -treated			
				HCT116	HT29	LoVo	SW480	HCT116	HT29	LoVo	SW480
				hsa-miR-921	7.26E-02	/	-1.89	1,513	968	3,656	2,338
hsa-miR-422a	7.26E-02	/	-1.82	76	125	85	18	9	43	11	24
hsa-miR-29b-3p	7.27E-02	/	2.01	178	405	291	135	1,000	1,071	218	1,775
hsa-miR-885-5p	7.29E-02	/	-1.87	3	36	19	11	19	0	0	0
hsa-miR-224-3p	7.46E-02	/	0.96	21	8	26	17	51	27	35	24
hsa-miR-550a-3-5p	7.56E-02	/	-2.91	19	23	42	14	1	12	0	0
hsa-miR-105-5p	7.59E-02	/	-2.31	38	10	40	38	4	1	20	0
hsa-miR-2682-3p	7.64E-02	/	3.97	0	2	1	3	9	34	8	42
hsa-miR-378d	7.67E-02	/	-1.20	929	559	777	806	299	132	733	174
hsa-miR-379-5p	7.69E-02	/	-1.72	174	3	126	365	0	0	203	0
hsa-miR-197-3p	7.75E-02	/	-0.92	118	281	109	172	93	78	121	70

miRNA	p-value	FDR	Log2 (FC)	Untreated				<i>F. nucleatum</i> -treated			
				HCT116	HT29	LoVo	SW480	HCT116	HT29	LoVo	SW480
				hsa-miR-146b-5p	7.89E-02	/	-1.75	3,821	1,090	4,040	3,742
hsa-miR-135b-5p	7.98E-02	/	-3.67	71	22	106	21	0	4	14	0
hsa-miR-7975	8.09E-02	/	-2.02	62	136	81	25	2	16	18	39
hsa-miR-15b-5p	8.16E-02	/	0.62	1,681	1,256	1,038	1,952	2,971	1,545	2,505	2,104
hsa-miR-10b-5p	8.16E-02	/	1.24	23	127	38	97	155	155	217	141
hsa-miR-152-3p	8.28E-02	/	3.90	5	5	3	10	212	7	20	102
hsa-miR-4281	8.37E-02	/	0.90	93	30	91	50	128	107	89	166
hsa-miR-345-5p	8.69E-02	/	0.98	12	19	10	39	40	46	44	29
hsa-miR-194-5p	8.72E-02	/	-1.53	1,326	1,274	2,771	2,157	95	44	2,318	148
hsa-miR-223-5p	8.74E-02	/	-2.52	142	42	146	110	0	2	74	1
hsa-miR-450a-1-3p	8.89E-02	/	-6.58	6	52	4	0	0	1	0	0

miRNA	p-value	FDR	Log2 (FC)	Untreated				<i>F. nucleatum</i> -treated			
				HCT116	HT29	LoVo	SW480	HCT116	HT29	LoVo	SW480
				hsa-miR-25-5p	8.92E-02	/	-1.17	32	17	22	54
hsa-miR-431-5p	8.98E-02	/	-2.21	61	10	30	132	2	7	35	6
hsa-miR-6813-5p	9.02E-02	/	2.24	0	0	0	9	2	2	2	37
hsa-miR-7706	9.28E-02	/	-2.99	78	8	18	5	13	0	1	0
hsa-miR-3074-3p	9.36E-02	/	3.33	6	0	0	2	9	50	2	20
hsa-miR-7-1-3p	9.41E-02	/	0.50	32	47	38	46	82	52	54	44
hsa-miR-361-5p	9.44E-02	/	-1.62	354	773	1,061	178	137	154	320	156
hsa-miR-675-3p	9.51E-02	/	3.67	0	8	2	14	122	90	27	56
hsa-miR-378a-3p	9.75E-02	/	-0.98	1,960	1,225	1,732	1,834	819	359	1,723	515

Abbreviations: FDR, false discovery rate; FC, fold change

Supplementary Table 2: Potential targets of miR-21 from 9 well-known prediction programs using miRWalk2.0 database.

Gene	DIANAmT	miRanda	miRDB	miRWalk	RNAhybrid	PICTAR5	PITA	RNA22	Targetscan	SUM
KCNMB2	1	1	1	1	0	1	1	1	1	8
LUM	1	1	1	1	0	1	1	1	1	8
MSH2	1	1	1	1	0	1	1	1	1	8
TRPM7	1	1	1	1	0	1	1	1	1	8
CHD7	1	1	1	1	1	1	0	1	1	8
RASA1	1	1	0	1	1	1	1	1	1	8
C17orf39	1	1	1	1	1	1	1	0	1	8

Supplementary Table 3: The correlation of *F nucleatum* DNA level, miR-21 expression and clinicopathological factors in CRC patients.

Characteristics	Total (n)	Tissue <i>F nucleatum</i>			Tissue miR-21			Tissue <i>F nucleatum</i> /miR-21			
		Negative	Low	High	Down	Up	L/L	L/H or	H/H		
		(n)	(n)	(n)	(n)	(n)	(n)	(n)	H/L (n)	(n)	
				<i>P</i> -value			<i>P</i> -value			<i>P</i> -value	
All cases (n, %)	90	22 (24.4)	34 (37.8)	34 (37.8)		45 (50)	45 (50)		34 (37.8)	33 (36.7)	23 (25.6)
Age (years)					0.282			0.832			0.818
< 70	51	15	16	20		25	26		18	20	13
≥ 70	39	7	18	14		20	19		16	13	10
Gender					0.355			0.832			0.438
Female	39	8	18	13		19	20		14	17	8
Male	51	14	16	21		26	25		20	16	15
Tumor location					0.378			0.765			0.181
Right hemicolon	23	9	8	6		13	10		13	4	6

Characteristics	Total (n)	Tissue <i>F nucleatum</i>			Tissue miR-21			Tissue <i>F nucleatum</i> /miR-21			
		Negative	Low	High	Down	Up	L/L	L/H or	H/H		
		(n)	(n)	(n)	(n)	(n)	(n)	(n)	H/L (n)	(n)	
				<i>P</i> -value			<i>P</i> -value			<i>P</i> -value	
Left hemicolon	31	6	13	12		15	16		10	14	7
Rectum	36	7	13	16		17	19		11	15	10
Tumor size (cm)					0.934			0.399			0.828
< 5	46	12	17	17		21	25		17	16	13
≥ 5	44	10	17	17		24	20		17	17	10
Differentiation					0.942			1.000			0.888
Well-moderate	80	20	30	30		40	40		30	30	20
Poor	10	2	4	4		5	5		4	3	3
T					0.027			0.438			0.437
Tis – T2	17	9	6	4		8	11		7	9	3

Characteristics	Total (n)	Tissue <i>F nucleatum</i>			Tissue miR-21			Tissue <i>F nucleatum</i> /miR-21			
		Negative	Low	High	Down	Up	L/L	L/H or	H/H		
		(n)	(n)	(n)	(n)	(n)	(n)	(n)	H/L (n)	(n)	
				<i>P</i> -value			<i>P</i> -value			<i>P</i> -value	
T3 – T4	73	13	28	30		37	34		27	24	20
N					0.163			0.673			0.654
N0	45	13	20	13		22	24		19	17	10
N1 – N2	45	9	14	21		23	21		15	16	13
M					0.447			0.006			0.018
Absence	82	21	32	29		45	37		34	30	18
Presence	8	1	2	5		0	8		0	3	5
TNM stage					0.520			0.008			0.156
0/I	15	6	5	4		6	9		5	7	3
II	30	7	14	9		16	14		14	9	7

Characteristics	Total (n)	Tissue <i>F nucleatum</i>			Tissue miR-21			Tissue <i>F nucleatum</i> /miR-21		
		Negative	Low	High	Down	Up	L/L	L/H or	H/H	
		(n)	(n)	(n)	(n)	(n)	(n)	(n)	H/L (n)	(n)
III	37	8	13	16	23	14	15	14	8	
IV	8	1	2	5	0	8	0	3	5	
FOBT					0.162		0.286		0.966	
Negative	40	13	14	13	18	22	15	15	10	
Positive	46	7	19	20	26	20	18	16	12	
NA	4									
Serum CEA (µg/L)					0.423		0.310		0.098	
≤ 5.9	53	11	23	19	29	24	20	23	10	
> 5.9	28	7	8	13	12	16	10	7	11	

Characteristics	Total (n)	Tissue <i>F nucleatum</i>			Tissue miR-21			Tissue <i>F nucleatum</i> /miR-21			
		Negative	Low	High	Down	Up	L/L	L/H or	H/H		
		(n)	(n)	(n)	(n)	(n)	(n)	(n)	H/L (n)	(n)	
				<i>P</i> -value			<i>P</i> -value			<i>P</i> -value	
P53 status					0.892		0.799				0.872
Negative	21	5	8	8		11	10	8	8	5	
Positive	57	13	19	25		28	29	20	20	17	
NA	12										
Lymphatic- invasion					0.031		0.528				0.300
Negative	27	11	9	7		15	12	13	9	5	
Positive	52	8	19	25		25	27	17	18	17	
NA	11										
Nerve-invasion					0.213		0.064				0.788

Characteristics	Total (n)	Tissue <i>F nucleatum</i>			Tissue miR-21			Tissue <i>F nucleatum</i> /miR-21		
		Negative	Low	High	Down	Up	L/L	L/H or	H/H	
		(n)	(n)	(n)	(n)	(n)	(n)	(n)	H/L (n)	(n)
Negative	21	8	6	7	7	14	7	7	7	
Positive	58	11	22	25	33	25	23	20	15	
NA	11									
Smoking					0.840		0.193			0.378
Absence	80	19	30	31	40	40	30	29	21	
Presence	5	1	3	1	4	1	3	2	0	
NA	5									
Diabetes					0.789		0.893			0.671
Absence	70	17	26	27	36	34	26	27	17	
Presence	15	3	7	5	8	7	7	4	4	

Characteristics	Total (n)	Tissue <i>F nucleatum</i>			Tissue miR-21			Tissue <i>F nucleatum</i> /miR-21		
		Negative	Low	High	Down	Up	L/L	L/H or	H/H	
		(n)	(n)	(n)	(n)	(n)	(n)	(n)	H/L (n)	(n)
				<i>P</i> -value			<i>P</i> -value			<i>P</i> -value
NA	5									
Appendectomy					1.000		0.026			0.234
Absence	79	19	30	30		38	41	29	29	21
Presence	6	1	3	2		6	0	4	2	0
NA	5									

Abbreviations: NA, not available.

Supplementary Table 4: Primer sequences used in this study.

Primers	Sequence 5'-3'	Purpose
<i>F nucleatum</i>	Forward primer:	qPCR
	CAACCATTACTTTAACTCTACCATGTTCA	
	Reverse primer:	
	GTTGACTTTACAGAAGGAGATTATGTAAAAATC	
<i>PGT</i>	FAM probe:	qPCR
	GTTGACTTTACAGAAGGAGATTA	
	Forward primer:	
	ATCCCCAAAGCACCTGGTTT	
<i>U6</i>	Reverse primer:	qPCR
	AGAGGCCAAGATAGTCCTGGTAA	
	FAM probe:	
	CCATCCATGTCCTCATCTC	
<i>U6</i>	Forward primer:	qPCR
	GTGCTCGCTTCGGCAGCACAT	
	Reverse primer:	
	GTTTAAGCACTTCGCAAGGTA	

	Forward primer:	
	TAGCTTATCAGACTGATGTTGA	
miR-21		qPCR
	Reverse primer:	
	CAGTGCGTGTCGTGGAGT	
	Forward primer:	
	TGAGGTAGTAGGTTGTATAGTT	
let-7a		qPCR
	Reverse primer:	
	CAGTGCGTGTCGTGGAGT	
	Forward primer:	
	ATCACATTGCCAGGGATTCC	
hsa-miR-23a-3p		qPCR
	Reverse primer:	
	CAGTGCGTGTCGTGGAGT	
	Forward primer:	
	ATCACATTGCCAGGGATTACC	
hsa-miR-23b-3p		qPCR
	Reverse primer:	
	CAGTGCGTGTCGTGGAGT	
	Forward primer:	
	TGAGGTAGTAGATTGTATAGTT	
hsa-let-7f-5p		qPCR

	Reverse primer:	
	CAGTGCGTGTCGTGGAGT	
	Forward primer:	
	TGAGGTAGTAGTTTGTGCTGTT	
hsa-let-7i-5p		qPCR
	Reverse primer:	
	CAGTGCGTGTCGTGGAGT	
	Forward primer:	
	GATCCGCTGATGTGCACCGACAAGCTTCCTGTCAGACTT	Lentivirus
	GTCGGTGACATCAGCTTTTTG	packaging
shRNA-p50	Reverse primer:	and
	AATTCAAAAAGCTGATGTGCACCGACAAG	transduction
	TCTGACAGGAAGCTTGTCGGTGACATCAGCG	
	Forward primer:	
	GATCCGCATGGAACCATGGACACTCTTCCTGTCAGAAGT	Lentivirus
	GTCCATGGTTCCATGC TTTTGG	packaging
shRNA-p65	Reverse primer:	and
	AATTCAAAAAGCATGGAACCATGGACACTTCTGACAGG	transduction
	AAGAGTGTCATGGTTCCATGCG	
shRNA-NC	Forward primer:	Lentivirus
		packaging

	GATCCGAAGCCAGATCCAGCTTCCCTTCCTGTCAGAGGA	and
	AGCTGGATCTGGCTTCTTTTTG	transduction
	Reverse primer:	
	AATTCAAAAAGAAGCCAGATCCAGCTTCCCTCTGACAGG	
	AAGGGAAGCTGGATCTGGCTTCG	
	Forward primer:	
hsa-miR-21	ATCCAGCAGCGGTTGAACTC	ChIP
promoter	Reverse primer:	
	TCCTCCAATTTAAGGCAGAAC	
	Forward primer:	
hsa-miR-21 10 kb	AGGCGGTTGTTGGCTTCAG	ChIP
upstream	Reverse primer:	
	GACCCAGAGAGTTCTATCAATTGA	
	Forward primer:	
	GGGGTACCGGAGGACTCCGGAGGACTCCGGAGGACTCC	
pGL3-WT (hsa-	GGAGGACTCCGGAGGACTCCGGAGGACTCCCGG	Luciferase
miR-21)	Reverse primer:	activity assay
	CCGCTCGAGGGAGTCCTCCGGAGTCCTCCGGAGTCCTCC	
	GGAGTCCTCCGGAGTCCTCCGGAGTCCTCCCC	

	Forward primer:	
pGL3-MT (hsa-miR-21)	GGGGTACCCTGACGGCGACTGACGGCGACTGACGGCGA	
	CTGACGGCGACTGACGGCGACTGACGGCGA CGG	Luciferase activity assay
	Reverse primer:	
	CCGCTCGAGTCGCCGTCAGTCGCCGTCAGTCGCCGTCAG	
	TCGCCGTCAGTCGCCGTCAGTCGCCGTCAGCC	
	Forward primer:	
TLR4	GGATGAGGACTGGGTAAGGAATGA	qPCR
	Reverse primer:	
	AGCGGCTCTGGATGAAGTGC	
	Forward primer:	
TLR2	GCGTGGCCAGCAGGTTTCAG	qPCR
	Reverse primer:	
	GAGCCAGGCCACATCATTTC	
	Forward primer:	
MYD88	GCCGCCGATGGTGGTGGTTGT	qPCR
	Reverse primer:	
	TTGGTGCAGGGTTGGTGTAGTCG	

	Forward primer:	
	GTGGCCGGTGCTGCTGTTGC	
RASA1		qPCR
	Reverse primer:	
	TGGCCACCTGTTCCCTCCTCGTATT	
	Forward primer:	
	TGTAGTTGAGGTCAATGAAGGG	
GAPDH		qPCR
	Reverse primer:	
	ACATCGCTCAGACACCATG	
	Forward primer:	
	AATCACACTCCTGCGTCATACAT	
KCNMB2		qPCR
	Reverse primer:	
	TCCCCGGAAGAAGTCAGGTTA	
	Forward primer:	
	GGGTGTTAAAATGTCCGCAGTTGA	
LUM		qPCR
	Reverse primer:	
	GTTCCCCATGTCTCCAGCAGTCT	
	Forward primer:	
MSH2		qPCR
	GGGTGTTAAAATGTCCGCAGTTGA	

	Reverse primer:	
	GTTTCCCATGTCTCCAGCAGTCT	
	Forward primer:	
	GGTTCCTCTTCTGGTGCCTTATTC	
TRPM7		qPCR
	Reverse primer:	
	TGGTTGGTGGGGATGACAGAT	
	Forward primer:	
	GAACCGCCCGACCTCTCCTCCATA	
CHD7		qPCR
	Reverse primer:	
	TGCCGTCCACACTCCCACCACTCT	
	Forward primer:	
	ATCCCGCCGCCGCCATCAA	
C17orf39		qPCR
	Reverse primer:	
	CAAAGGTAAGAGTTCCCCGTGTCC	
	Forward primer:	
	TAAAGCTGGAAAGGGACGAACT	
PTEN		qPCR
	Reverse primer:	
	ATAGCGCCTCTGACTGGGAATA	

	Forward primer:	
	CGAGCCCCAGATTATTGCCAGAG	
RECK		qPCR
	Reverse primer:	
	GCCTAAGCCAACCCAGCCATCAGA	
	Forward primer:	
	TGGCAGTGGCAGTTCGTTAGTTGT	
SPRY1		qPCR
	Reverse primer:	
	TGTCCGAGGAGCAGGTCTTTCA	
	Forward primer:	
	ACGGCGGGCCAGGAGGACTACGA	
RHOB		qPCR
	Reverse primer:	
	TGGGCACATTGGGACAGAAG	

Supplementary Figure Legends

Supplementary Figure 1: *F nucleatum* promotes CRC cell proliferation

a) HCT116 and LoVo cells were incubated with PBS, *E coli* DH5 α or *F nucleatum*. The cell proliferation was evaluated by CCK-8 assay after treatment at 6h, 24 and 48 hr. (n = 3. **P* < 0.05, ***P* < 0.01, ****P* < 0.001). b) The cell cycle distribution of treated or control cells was determined by flow cytometry-based assay after treatment at 48 hr. These results are representative of at least three independent experiments.

Supplementary Figure 2: *F nucleatum* promotes CRC invasion

HCT116 and LoVo cells were incubated with PBS, *E coli* DH5 α or *F nucleatum*. Wound healing assay was performed to evaluate the invasion capability of treated or control cells (10 \times).

Supplementary Figure 3: *F nucleatum* promotes CRC development in vivo

The *F nucleatum*-treated LoVo cells were subcutaneously injected into male BALB/C nude mice and generated the xenograft animal model. a) The representative images of xenograft mice (n = 5) and immunostaining for Ki-67 (200 \times) in xenograft tumor tissues. b) Tumor growth curve and tumor weight after DH5 α , *F nucleatum* or PBS treatment (n = 5. ***P* < 0.01 by one-way analysis of variance (ANOVA) and Bonferroni's multiple comparison test). Bars represent standard deviation (SD).

Supplementary Figure 4: *F nucleatum* did not promote CRC apoptosis in vivo

The representative immunostaining for TUNEL (200 \times) in xenograft tumor tissues (HCT116 and LoVo cells)

Supplementary Figure 5: *F nucleatum* promotes tumorigenicity in *Apc*^{Min/+} mouse

a) Representative image of a small intestine of APC^{Min/+} mice with or without *F nucleatum* treatment (n = 10). b-d) On 20 weeks, *F nucleatum*-treated APC^{Min/+} mice showed slight but no significant increase in the tumor numbers, tumor size and tumor load in small intestine (n = 10, Mann-Whitney *U* test).

Supplementary Figure 6: The validation of *F nucleatum*-induced miRNA in HCT116 and LoVo cells

a) qRT-PCR showed expression alteration of several candidates (let7f-5p, let7i-5p, miR23a-3p, let7a-5p, miR23b-3p, and miR21-5p) in *F nucleatum*-treated HCT116 cells and control cells. b) qRT-PCR showed expression alteration of several candidates in *F nucleatum*-treated LoVo cells and control cells. All results are representative of triplicate experiments (* $P < 0.05$, ** $P < 0.01$ by unpaired Student's t test. NS, no significance). Results represent means values \pm SD.

Supplementary Figure 7: *F nucleatum* infection showed less impact on miR21a^{-/-} mice

a) miR-21 expression in normal epithelial cells and CRC cells (** $P < 0.01$, *** $P < 0.001$ by unpaired Student's t test. NS, no significance). Results represent means values \pm SD). b) Hematoxylin and eosin (H&E) stains have been used for recognizing morphologic changes of CRC tissues from *F nucleatum*-treated miR-21a wild type (WT, miR-21^{wt}) or knockout (KO, miR21a^{-/-}) mice. c) A representative small intestine in *F nucleatum*-treated miR-21^{wt} or miR21a^{-/-} mice after 20 weeks was showed in the left upper picture. The red arrows indicated the positive location. On 20 weeks, *F nucleatum*-treated miR21a^{-/-} mice showed slight but no significant increase in the tumor number, tumor size and tumor load of small intestine (Mann-Whitney U test. $n = 7$ mice per group).

Supplementary Figure 8: *F nucleatum* affect several already proved miR-21 targets.

Several already evidenced targets of miR-21 (PTEN, RECK, SPRY1 and RHOB)¹ was tested in HCT116 and LoVo cells with or without *F nucleatum*-treatment. The mRNA levels of these miR-21 targets were measured by qRT-PCR. All bars represent the mean values \pm SD. All results are representative of triplicate experiments (** $P < 0.01$, *** $P < 0.001$ by unpaired Student's t test. NS, no significance).

Supplementary Figure 9: Validation of miR-21 putative targets in HCT116 cells.

F nucleatum-treated HCT116 cells were incubated with miR-21 mimics, inhibitors or scramble controls. The expression of potential miR-21 target genes were measured by qRT-PCR. All bars represent the mean values \pm SD. All results are representative of triplicate experiments ($**P < 0.01$, $***P < 0.001$ by unpaired Student's *t* test. NS, no significance).

Supplementary Figure 10: Validation of miR-21 putative targets in LoVo cells.

F nucleatum-treated LoVo cells were incubated with miR-21 mimics, inhibitors or scramble controls. The expression of potential miR-21 target genes were measured by qRT-PCR. All bars represent the mean values \pm SD. All results are representative of triplicate experiments ($*P < 0.05$, $**P < 0.01$, $***P < 0.001$ by unpaired Student's *t* test. NS, no significance).

Supplementary Figure 11: silence of NF κ B impaired the *F nucleatum*'s oncogenic effect on cell proliferation and invasion in HCT116 cells.

a) CCK-8 assay showed silence of NF κ B significantly impaired the *F nucleatum*'s oncogenic effect on cell proliferation ($*P < 0.05$ by unpaired Student's *t*-test. Bars represent SD of three experiments). b) Wound healing assay showed silence of NF κ B impaired the invasion capability of *F nucleatum*-treated cells (10 \times)

Supplementary Materials and Methods

Patients and specimen collection

We used 2 independent cohorts of CRC tissues. For the expression correlation analysis, we used 90 fresh frozen matched cancer and normal samples obtained from Six People's Hospital Affiliated to Shanghai Jiao Tong University from 2012 to 2013. For the survival analysis, we used 125 fresh frozen cancer tissues, which were collected at the Mie University, Japan. Written informed consent was obtained from all patients, and the study was approved by the Institutional Review Boards of all participating institutions.

Bacterial strain and culture conditions

The *F nucleatum* strain was obtained from American type culture collection (ATCC, *F nucleatum* subsp. *nucleatum* ATCC 25586) and was cultured as described previously^{2,3}. In brief, *F nucleatum* was grown in Columbia blood agar supplemented with 5 µg/ml haemin, 5% defibrinated sheep blood (5%), and 1 µg/ml vitamin K1 (Sigma-Aldrich, St. Louis., MO, USA) in an anaerobic glove box with 85% N₂, 10% H₂, and 5% CO₂ at 37°C. The *E coli* Strain DH5a (Invitrogen, Carlsbad, CA, USA) was propagated in Luria-Bertani (BD Biosciences, Difco, MD, USA) medium aerobically at 37°C.

Cell culture

The CRC cell lines (HCT116, SW480, HT29, Caco2, LoVo, SW620, DLD1, RKO, Colo205) and IEC were provided by the American Type Culture Collection (ATCC, Manassas, VA, USA). The human normal colon epithelial cell line NCM460 was obtained from the INCELL Corporation (San Antonio, TX, USA). All of the cell lines were cultured in appropriate conditions as described previously^{4,5}.

Cell proliferation assays

For the cell proliferation analysis, resuspension solution of HCT116 and LoVo cells were seeded at 1×10^4 per well in the 24-well plates with 2 ml complete medium. Cells were incubated with *F nucleatum* or

DH5 α at an multiplicity of infection (MOI) of 1000:1. Cells treated with PBS were set as negative control. Cells number counts were performed using a hemocytometer at 6 hr, 24 hr and 48 hr. Each test was repeated in triplicate.

Wound healing assays

Before the experiments, the back of each 6-well plate was marked out to set a unified location. CRC cells (HCT116 and LoVo, 5×10^5 per well) were left to grow until confluent and wounded with a pipette tip. Then the cells of each well were co-incubated with *F nucleatum* or DH5 α at an MOI of 1000:1. Cell images were taken at 6, 24 hr, and 48 hr. The wound size of each well was calculated as the distance between the edges.

Cell growth assays

Cells number counts were performed using a hemocytometer. Cell viability was analyzed using a Cell Counting Kit according to the manufacturer's instruction (CCK-8, Dojindo, Kumamoto, Japan).

Cell cycle assays

CRC cells were harvested and incubated with 50 μ g/ml propidium iodide (PI, Sigma-Aldrich, St. Louis., MO, USA) followed by 100 μ g/ml Rnase A and 0.2% Triton X-100. The stained cells were measured by flow cytometry (BD Bioscience, San Jose, CA, USA).

Immunohistochemistry (IHC) and Western blotting (WB)

For IHC, Dako envision+dual link system-HRP (DAB+) (Dako, Carpinteria, CA) were used according to the manufacturer's instructions. For WB, cell extracts were collected using T-PER Tissue Protein Extraction Reagent (Thermo Fisher Scientific, Wilmington, DE, USA) and loaded on to the 10% polyacrylamide-SDS gels, followed by transfer of electrophoresed proteins onto nitrocellulose

membranes. The membranes were then blocked in 5% fat-free milk and incubated with the following primary and secondary antibodies. The probe proteins were detected using enhanced chemiluminescence according to manufacturer's instructions. All the antibodies were purchased from Abcam.

Plasmids, lentivirus shRNA construction

The specific siRNA targeting coding region of p65 or p50 was as follow: siRNA-p65, 5'-GCTGATGTGCACCGACAAG-3'; siRNA-p50, GCATGGAACCATGGACACT-3'. A non-targeting sequence (5'-GAAGCCAGATCCAGCTTCC-3') was set as negative control (NC). The DNA fragments containing loop-structure for specific short-hairpin RNA (shRNA) and restriction sites (the XhoI in the up position and the BamHI in the down position) were synthesized (Invitrogen, Carlsbad, CA, USA) and amplified. Then the gene fragments were cloned into the pSIH1-H1-copGFP shRNA Cloning and Expression Vector (System Biosciences (SBI), Mountain View, CA, USA).

Cell transfection with miR-21 mimics or inhibitors

Cells were cultured and transfected with miR-21 mimics or negative control chemical synthesis oligonucleotides (GenePharma Corp., Shanghai, China) using Lipofectamine 2000 reagent (Invitrogen, Carlsbad, CA, USA) in indicated concentrations according to the supplier's instructions.

*DNA extraction and *F nucleatum* quantification*

Genomic DNAs from clinical human frozen samples were extracted using QIAamp DNA Mini Kit (Qiagen, GmbH, Hilden, Germany). The Taqman assay was used to amplify *F nucleatum*. The custom-made primers of *F nucleatum* were provided by the TaqMan primer/probe sets (Applied Biosystems, Foster City, CA, USA)⁷. Amplification and detection of *F nucleatum* gene were performed using TaqMan Environmental Master Mix 2.0 (Applied Biosystems, Foster City, CA, USA) on the Applied Biosystems

7500 RT-PCR System⁸. The thermal cycles were 95°C for 10 minutes and 45 cycles of 15 seconds at 95°C and 1 minute at 60°C. The *PGT* gene was used as internal control.

miRNA/mRNA microarray

Total RNAs were extracted from 4 cell lines (HCT116, HT29, LoVo and SW480), which treated by *F nucleatum* or PBS by using RNeasy Mini Kit (Qiagen, GmbH, Hilden, Germany). μ Paraflo™ MicroRNA microarray Assay was done using miRBase version 21.0 by LC Sciences (LC Sciences, Houston, TX, USA). Briefly, 5 μ g total RNAs were 3'-extended with a poly (A) tail and then ligated with an oligonucleotide tag conjugating Cy3 dye staining. The RNAs were hybridized overnight to a μ Paraflo microfluidic chip containing complementary target microRNA from miRBase (<http://www.mirbase.org/>). Fluorescence images were measured with a GenePix 400B laser scanner (Molecular Device, Sunnyvale, CA, USA) and digitized with a Array-Pro image analysis software (Media Cybernetics, Silver Spring, MD, USA). The miRNA array data were calculated by firstly subtracting the background value and then normalizing the signals by locally-weighted regression. The express levels of miRNAs were designated as statistically significant when the two-tailed P value was less than 0.05. And signals lower than 500 were interpreted as false positive result. The mRNA expression profiling was determined in *F nucleatum*-treated and *F nucleatum*-untreated HCT116 cells using SurePrint G3 Human Gene Expression v2 Microarray (Agilent Technologies, Santa Clara, CA, USA). The statistically significant mRNAs were selected based on the fold change and adjusted P value less than 0.05.

Tumor xenograft study

HCT116 and LoVo cells were co-cultured with *F nucleatum*, DH5 α or PBS at an MOI of 1000:1 for 24 hr. Then cells were washed thrice with PBS and harvested by trypsinization. Cell resuspension solution were then mixed with *F nucleatum*, DH5 α or PBS at an MOI of 20:1 and were injected (100 μ l per mouse) subcutaneously into the right flank of 6-week-old male nude mice (BALB/C, Shanghai, Chinese Academy of Sciences, China). 3 hr after hypodermic injection, all mice were intraperitoneally injected

with 150 mg/kg piperacillin to kill bacteria as described previously⁹. Nude mice were raised in the specific-pathogen-free (SPF) conditions with autoclaved food and water. The tumor volumes (Vol) were monitored at set times and were calculated as follows: $Vol = 1/2(\text{length-diameter} \times \text{width-diameter}^2)$. Mice were euthanized on day 39 and the tumor weight was measured. Tissues were snap frozen in liquid nitrogen and stored at -80 °C. Experiments were performed with 6 mice (HCT116 cells) or 5 mice (LoVo cells) in each group.

Cell apoptosis Assay

The tumor cell apoptosis was detected by the terminal deoxynucleotidyl transferase-mediated dUTP-biotin nick end labeling assay (TUNEL) assay. Briefly, 5 μ m-thick formalin-fixed paraffin-embedded (FFPE) section of tumor xenograft was stained using the In Situ Cell Death Detection Kit, POD (Roche Diagnostics GmbH, Mannheim, Germany) according to manufacturer's instructions. The cell nucleus was counterstained with hematoxylin. Slides were analyzed under a light microscope.

Mouse model

C57BL/6J-Adenomatous polyposis coli (APC)^{min}/J mice (APC^{min/+}) were provided from Nanjing Biomedical Research Institute of Nanjing University (NBRI). C57BL/6J miR-21 knockout (KO, miR-21a^{-/-}) and C57BL/6J wild-type (WT) mice were provided and bred as previously described¹⁰. All mice were housed and reared in SPF and barrier conditions with autoclaved food and water at the animal center of Shanghai Tenth People's Hospital Affiliated to Tongji University. The body weight of mice were measured every week.

For miR-21a^{-/-} mouse model, 8-9-week-old mice were additionally given two cycles of one single intraperitoneal injection of carcinogen azoxymethane (AOM) at 12 mg/kg body weight followed by five successive days of 2% dextran sodium sulfate (DSS) in the drinking water, and then were given regular drinking water. During the DSS intervention, the bacteria administration was suspended.

Before bacterial intragastric administration, APC^{min/+} or miR-21a^{-/-} mice were fed with 2 mg/ml streptomycin in the drinking water for 3 days to ensure the consistency of regular microbiota and facilitate *F nucleatum* colonisation. PBS-resuspended 10⁹ colony-forming units (CFU) *F nucleatum* or PBS were administered into 5-6 weeks APC^{min/+} or miR-21a^{-/-} male mice by gavage every day. To investigate the *F nucleatum*-induced gut tumor progression, bacteria or PBS administration was given for a period of 24 weeks. For *F nucleatum*-influenced survival, *F nucleatum*-treated APC^{min/+} or miR-21a^{-/-} mice were followed up until moribund. At the indicated time intervals, the mice were anaesthetized with 40mg/kg pentobarbital sodium and sacrificed for tumor statistics and histopathological analysis. Tissues were longitudinally opened and measured. The tumor numbers were counted and the tumour sizes (diameter) were quantified as <1 mm, 1-2 mm, 2-3 mm, > 3 mm. The algorithm of tumor load was the sum of every tumor diameter.

Enzyme linked immunosorbent assay (ELISA)

The mice serum was collected from each group and immediately stored at liquid nitrogen. The Quantification of serum cytokine was determined using Quantibody® Mouse Th17 Array 1 Kit (RayBiotech, Norcross, Georgia (GA), USA) following the manufacturers' protocol. The cytokines detected included the IFN-gamma, IL1 beta, IL10, IL12 p70, IL13, IL17A, IL17F, IL2, IL21, IL22, IL23 p19, IL28A, IL4, IL5, IL6, MIP3 alpha, TGF beta 1, and TNF alpha.

Cell transfection with miR-21 mimics or inhibitors

Cells were cultured and transfected with miR-21 mimics (sense: 5'-UAGCUUAUCAGACUGAUGUUGATT-3'; antisense: 5'-UCAACAUCAGUCUGAUAAGCUATT-3'), inhibitor (5'-UCAACAUCAGUCUGAUAAGCUATT-3') or negative control (NC, 5'-ACUAGUCGAUCUAUGUGUGAUATT-3') chemical synthesis oligonucleotides (GenePharma Corp., Shanghai, China) using Lipofectamine 2000 reagent (Invitrogen, Carlsbad, CA, USA) in indicated

concentrations according to the supplier's instructions. The efficiency after transfection was analysed using fluorescence microscopy.

Plasmids, lentivirus shRNA construction and transfection

The specific siRNA targeting coding region of p65 or p50 was as follow: siRNA-p65, 5'-GCTGATGTGCACCGACAAG-3'; siRNA-p50, GCATGGAACCATGGACACT-3'. A non-targeting sequence (5'-GAAGCCAGATCCAGCTTCC-3') was set as negative control (NC) The DNA fragments containing loop-structure for specific short-hairpin RNA (shRNA) and restriction sites (the XhoI in the up position and the BamHI in the down position) were synthesized (Invitrogen, Carlsbad, CA, USA) and amplified. Then the gene fragments were cloned into the pSIH1-H1-copGFP shRNA Cloning and Expression Vector (System Biosciences (SBI), Mountain View, CA, USA). Competent DH5 α was mixed with 10 μ l ligated products and grow in Super Optimal broth with Catabolite repression (SOC) culture medium. The positive clones in constructed plasmids were confirmed by sequencing. 293T cell was co-transfected with 4 μ l plasmid vector and 20 μ l pPACKH1 HIV Lentiviral Packaging Kit according to the protocol of SBI (Mountain View, CA, USA). After 48hr, the recombinant lentiviruses were harvested. HCT116 or LoVo cells were transfected with the recombinant shRNA lentiviruses at an MOI of 20 for subsequent experiments

Luciferase reporter assay

For the validation of the miR-21 target, the 3'UTR segment of RasA1 containing the wild-type (WT) or mutant (MT) target site for miR-21 was amplified by PCR from genome cDNA and inserted into the pGL3-Promoter Vector (Promega, Wisconsin (WI), USA). The CRC cell line HCT116 was transfected with the synthetic miR-21 mimics/miR-21 inhibitor/NC and co-transfected with the pGL3 plasmid and firefly luciferase report vector in 24-well plates using the Lipofectamine 2000 reagent (Invitrogen Corp., California (CA), USA). To verify if NF κ B could putatively bind to the miR-21 promoter, the WT or MT

DNA fragments of the miR-21 promoter were amplified and cloned into the pGL3-Promoter Vector. The control plasmid or reporter plasmid was co-transfected with Lv-shRNA-p65 vector into 293 cell using the Lipofectamine 2000 reagent. Luciferase assays were measured 48 hr after transfection using the Dual-Luciferase Reporter Assay System (Promega, WI, USA) according to the manufacturer's protocol, with the Renilla luciferase activity as a normaliser. The transfection efficiency data were normalized by dividing the Firefly luciferase activities with that of Renilla luciferase. The primers used were described in supplementary table S1. All PCR clones products were identified by DNA sequencing. Each assay was performed independently in triplicate.

Chromatin immunoprecipitation (ChIP)

ChIP reactions were performed using the ChIP Assay Kit (Millipore, Merck KGaA, Darmstadt, Germany) according to the manufacturer's operation manual. Briefly, HCT116 cells were treated with *F nucleatum* or PBS for 24 hours. The collected and resuspended cells were cross-linked with 1% formaldehyde at 37°C for 10 minutes and quenched by glycine. Cells were then resuspended in lysis buffer on ice for 10 minutes. The lysate were sonicated into 200-1000 base pairs. After centrifugation, the supernatant containing chromatin and magnetic beads was incubated with specific antibodies: anti-NFκB p65 (Santa Cruz Biotechnology) or normal mouse immunoglobulin G (IgG, Santa Cruz Biotechnology, Santa Cruz, CA, USA) at 37°C overnight for immunoprecipitation. The DNA/antibody/magnetic bead complexes were washed and eluted with low salt immune complex wash buffer following by high salt immune complex wash buffer, LiCl immune complex wash buffer and TE buffer. The purified chromatin DNA samples were measured with primers[26] for the promoter of hsa-miR-21 gene or 10 kb upstream regions of has-miR-21 by real-time PCR using the SYBR Premix Ex Taq (Takara Biotechnology, Dalian, China) with a 7500 Real-Time PCR System according to the manual supplied by Applied Biosystems (Carlsbad, CA, USA). Three independent reactions were performed.

Fluorescence in situ hybridization (FISH)

Localization of *F nucleatum* and miR-21 in CRC and adjacent normal tissues was performed by FISH on 5µm FFPE sections as described previously^{11, 12}. For the detection of miR-21, the digoxigenin-labeled Locked Nucleic Acid (LNA) mirCURY miRNA detection probe (miR-21: Digoxigenin-5'-TCAACATCAGTCTGATAAGCTA-3'-Digoxigenin, dilution ratio 1:100) was purchased from Exiqon (Vedbaek, Denmark). The small nuclear RNA U6 was set as positive control. For the detection of *F nucleatum*, the digoxigenin-labeled *F nucleatum* probe (Digoxigenin-5'-CGCAATACAGAGTTGAGCCCTGC-3'-Digoxigenin, dilution ratio 1:100) and universal bacterial probe (Digoxigenin-5'-GCTGCCTCCCGTAGGAGT-3'-Digoxigenin) were acquired from probeBase (<http://www.microbial-ecology.net/probebase/>) and synthesized by Sangon Biotech Company (Shanghai, China).

Statistical analyses

Differences of the quantitative data between two groups were performed using the unpaired or paired Student's t-test, Mann-Whitney U-test, or Dunnett's t-test, where appropriate. Comparisons of means among multiple groups were determined by one-way analysis of variance (ANOVA) tests. The relationships between the abundance of *F nucleatum* and the expression level of miR-21 was analyzed by using linear regression. The associations between the patient categorical characteristics were done using Pearson's Chi-square test or Fisher exact test, as appropriate. The median value was chosen as cutoff point. The impacts of clinical parameters were estimated by using univariate or multivariate Cox proportional hazards regression model analysis. The overall survival which was classed as the time from the first disease diagnosis to the date of death or last contact was designated as endpoints of interest. The Kaplan-Meier survival curves and log-rank tests were performed to determine the statistical analyses of overall survival. All P values were two-tailed and P values less than 0.05 were designated as significant difference (*P < 0.05, ** P < 0.01, *** P < 0.001). All statistical analyses were done by using the

GraphPad Prism 6 software (GraphPad software, Inc., San Diego, California, USA) and IBM SPSS Statistics 20.0 software (IBM, Inc., Chicago, Illinois, USA).

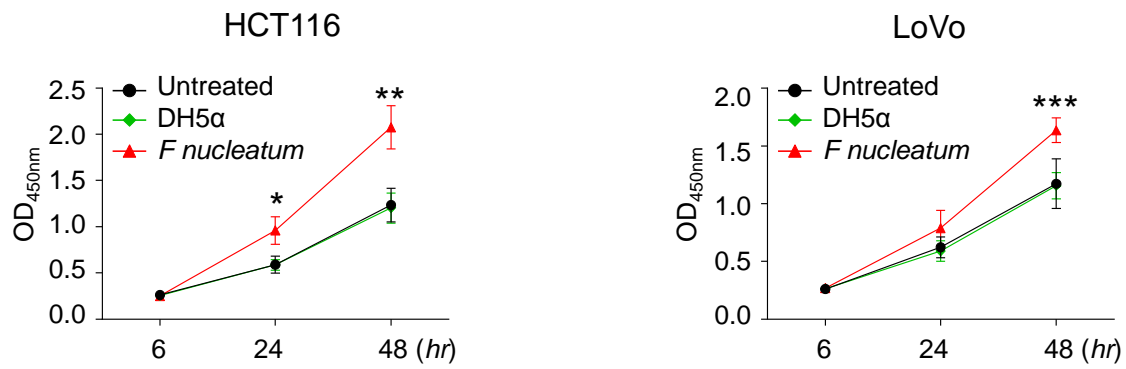
References

1. Jung EJ, Calin GA. The Meaning of 21 in the MicroRNA world: perfection rather than destruction? *Cancer Cell* 2010;18:203-5.
2. Kostic AD, Chun E, Robertson L, et al. *Fusobacterium nucleatum* potentiates intestinal tumorigenesis and modulates the tumor-immune microenvironment. *Cell Host Microbe* 2013;14:207-15.
3. Fardini Y, Wang X, Temoin S, et al. *Fusobacterium nucleatum* adhesin FadA binds vascular endothelial cadherin and alters endothelial integrity. *Mol Microbiol* 2011;82:1468-80.
4. Ma Y, Yang Y, Wang F, et al. Long non-coding RNA CCAL regulates colorectal cancer progression by activating Wnt/beta-catenin signalling pathway via suppression of activator protein 2alpha. *Gut* 2015.
5. Ma Y, Zhang P, Wang F, et al. Human embryonic stem cells and metastatic colorectal cancer cells shared the common endogenous human microRNA-26b. *Journal of cellular and molecular medicine* 2011;15:1941-54.
6. Livak KJ, Schmittgen TD. Analysis of relative gene expression data using real-time quantitative PCR and the 2(-Delta Delta C(T)) Method. *Methods* 2001;25:402-8.

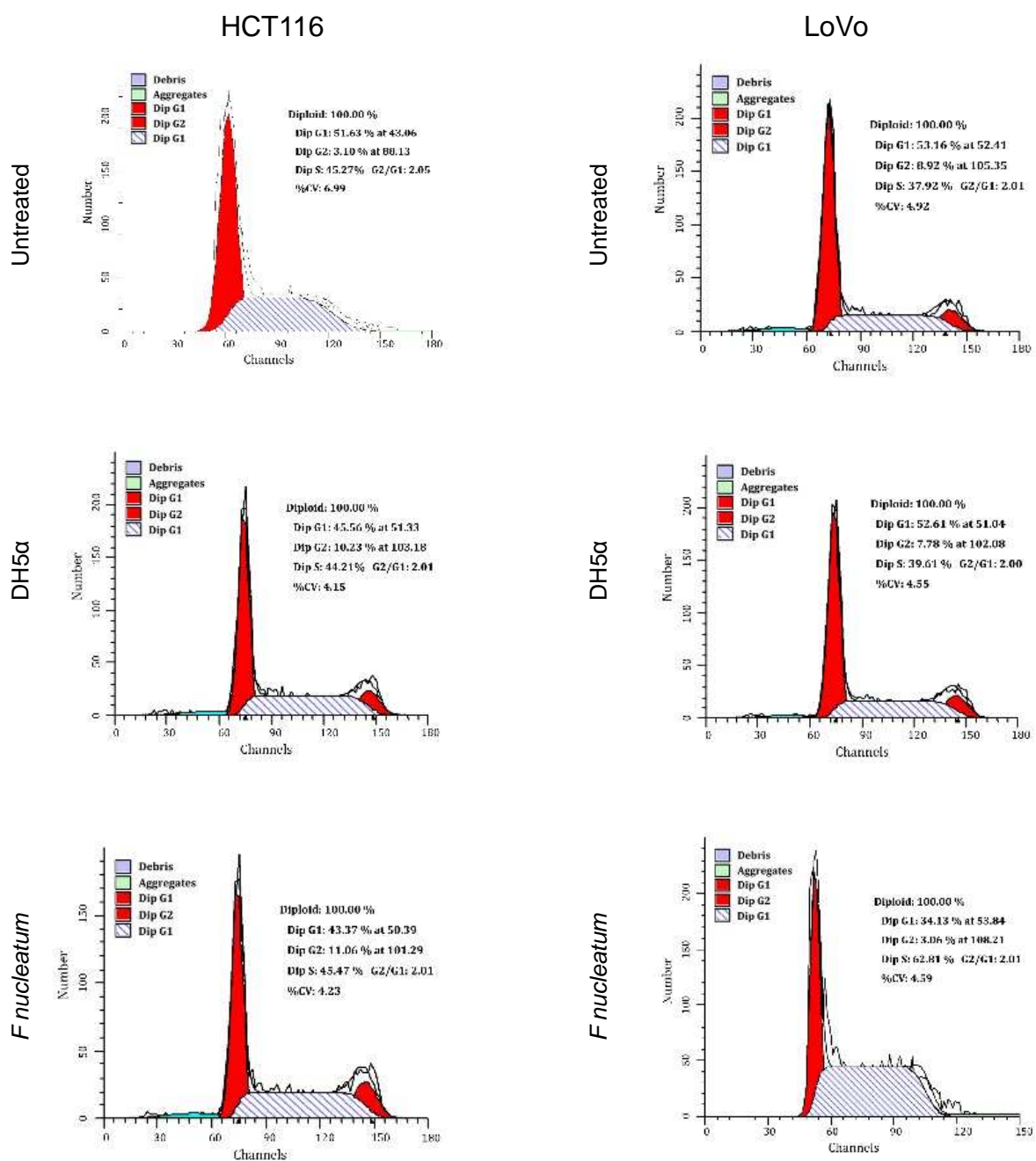
7. Mima K, Sukawa Y, Nishihara R, et al. *Fusobacterium nucleatum* and T Cells in Colorectal Carcinoma. *JAMA Oncol* 2015;1:653-61.
8. Tahara T, Yamamoto E, Suzuki H, et al. *Fusobacterium* in colonic flora and molecular features of colorectal carcinoma. *Cancer Res* 2014;74:1311-8.
9. Coughnoux A, Dalmaso G, Martinez R, et al. Bacterial genotoxin colibactin promotes colon tumour growth by inducing a senescence-associated secretory phenotype. *Gut* 2014;63:1932-42.
10. Shi C, Yang Y, Xia Y, et al. Novel evidence for an oncogenic role of microRNA-21 in colitis-associated colorectal cancer. *Gut* 2015.
11. Ma Y, Zhang P, Wang F, et al. miR-150 as a potential biomarker associated with prognosis and therapeutic outcome in colorectal cancer. *Gut* 2012;61:1447-1453.
12. Sigge A, Essig A, Wirths B, et al. Rapid identification of *Fusobacterium nucleatum* and *Fusobacterium necrophorum* by fluorescence in situ hybridization. *Diagn Microbiol Infect Dis* 2007;58:255-9.

Supplementary Figure 1

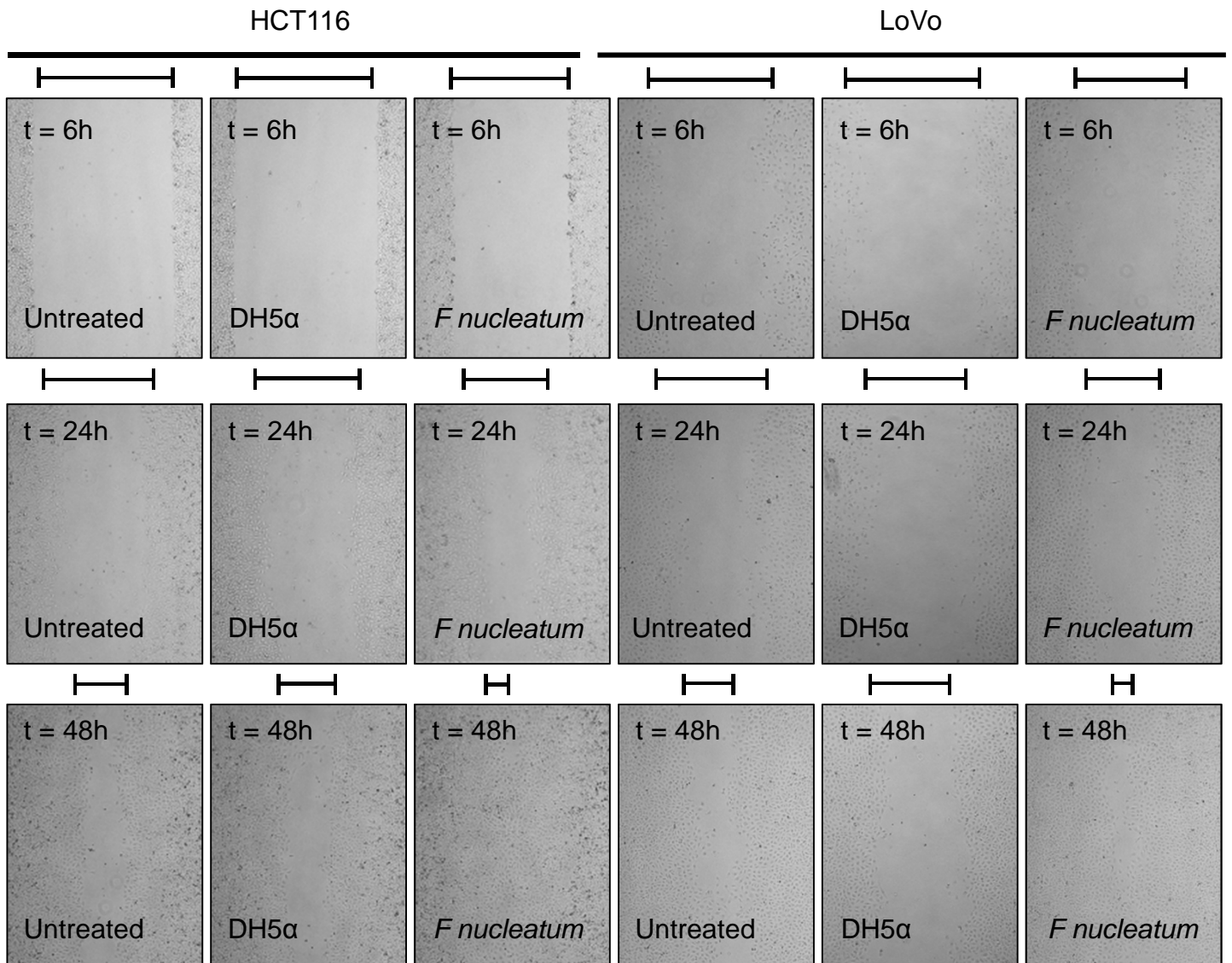
A



B

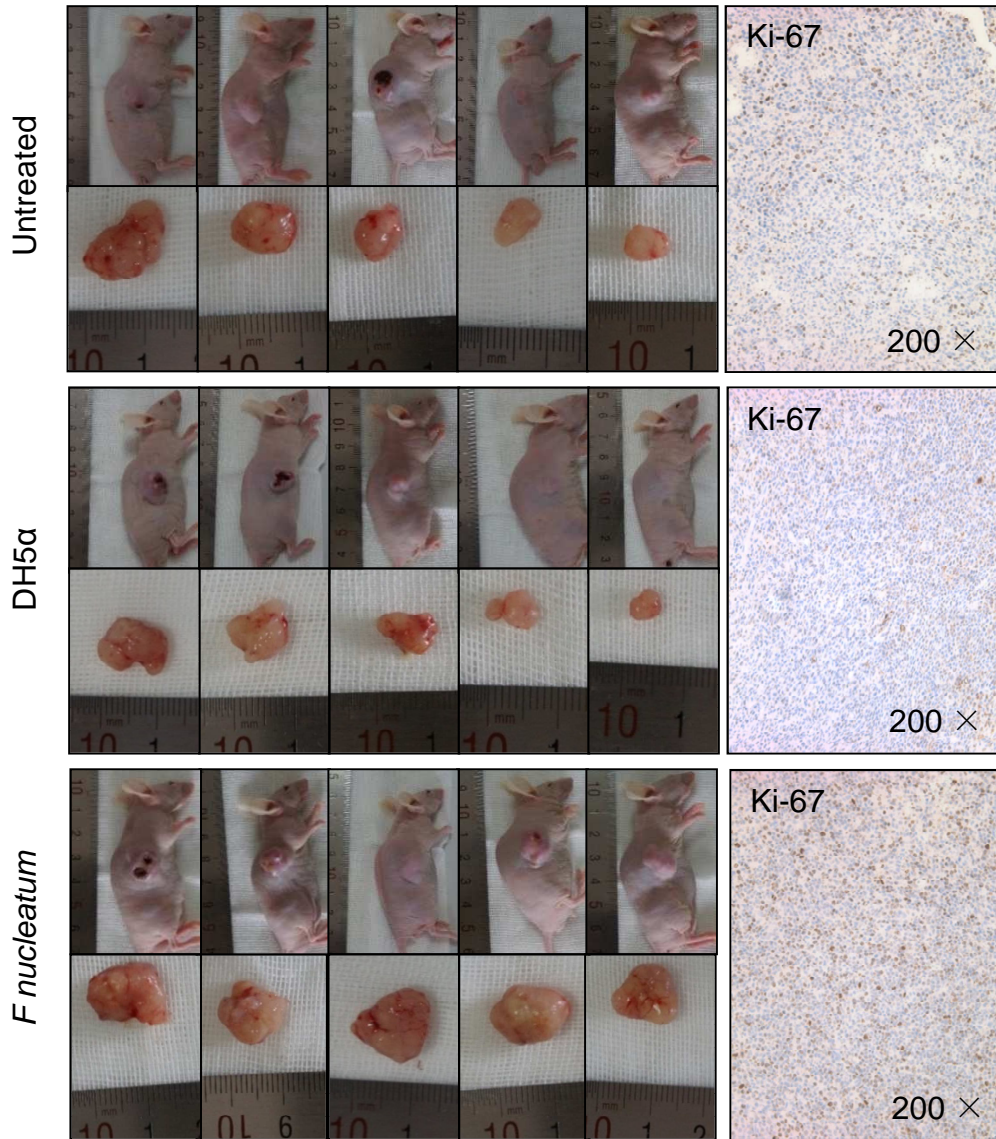


Supplementary Figure 2

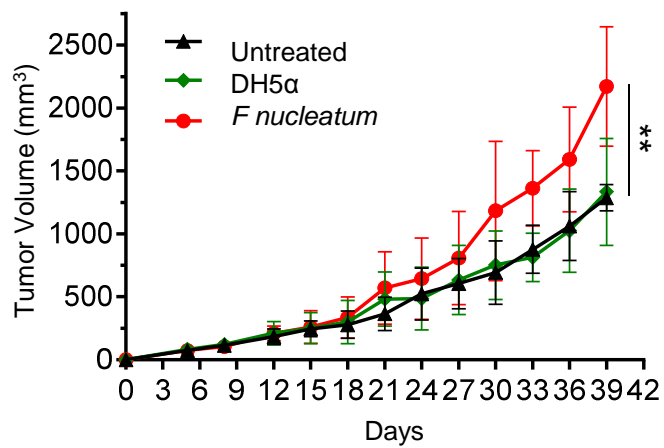


Supplementary Figure 3

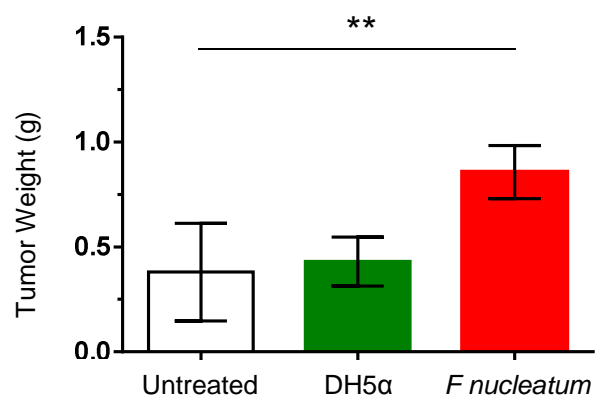
A



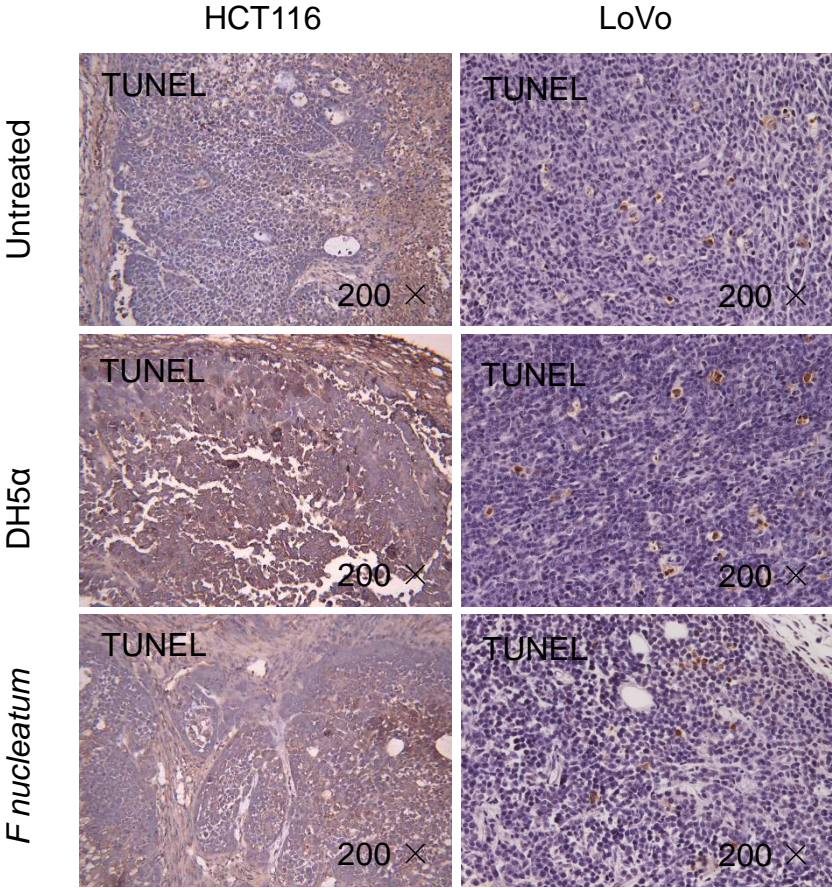
B



C



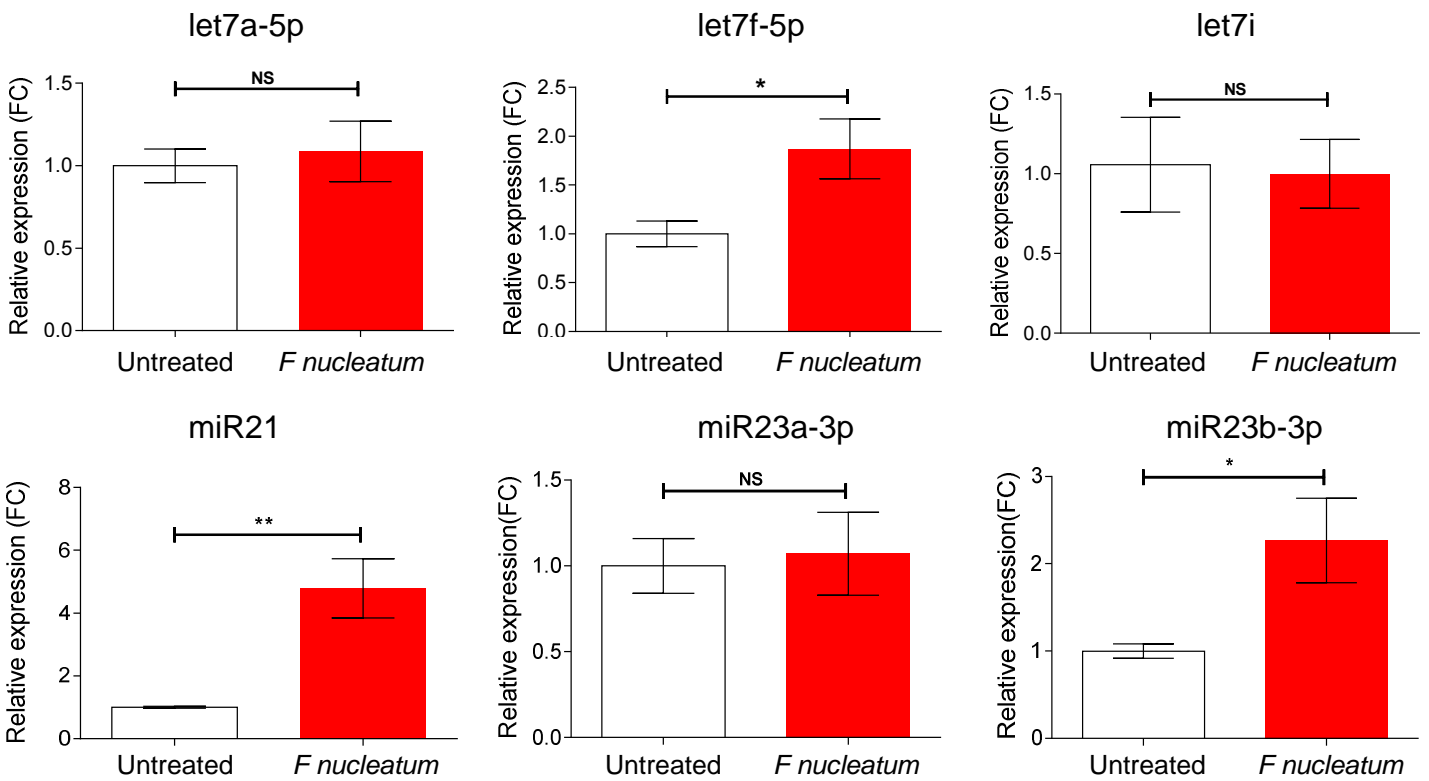
Supplementary Figure 4



Supplementary Figure 6

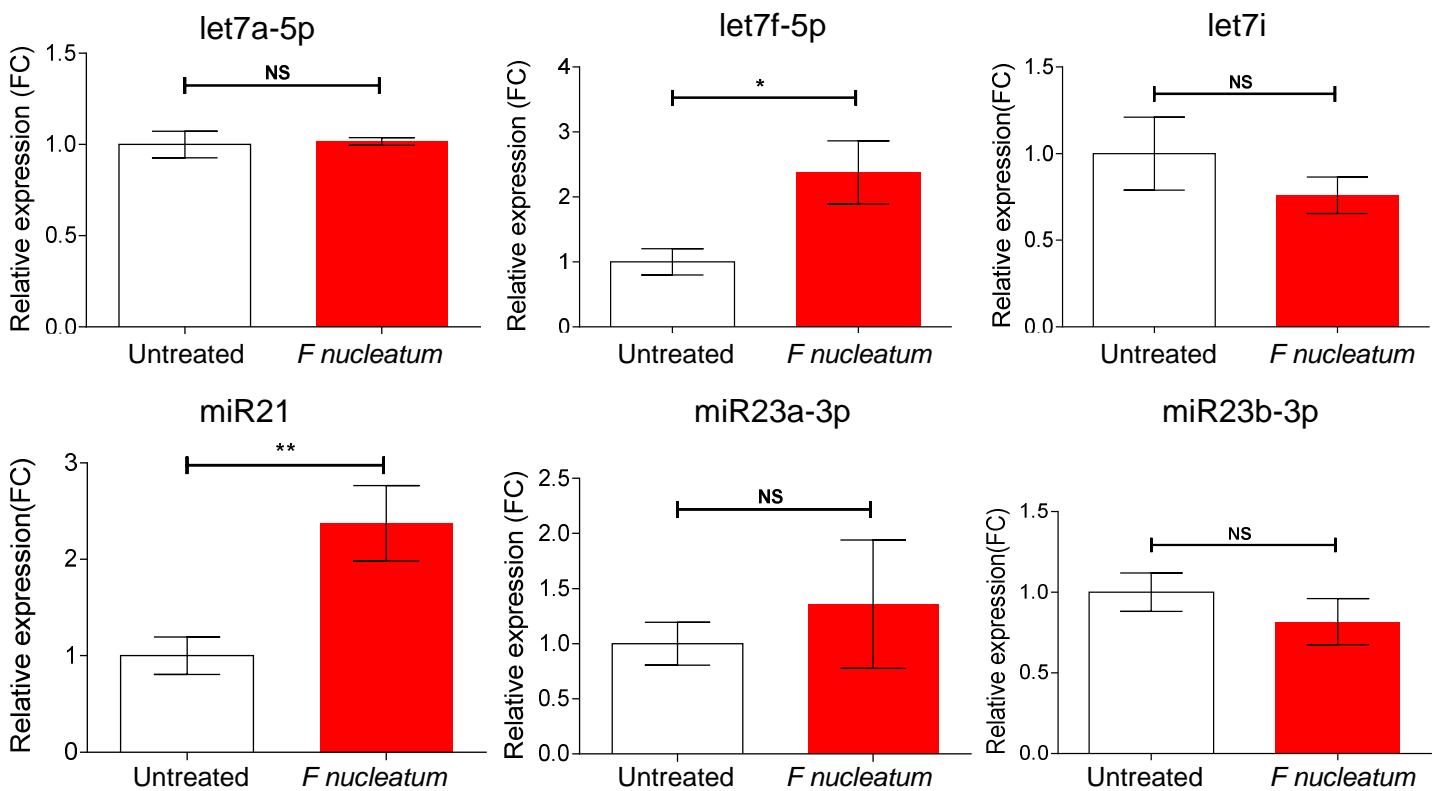
A

HCT116



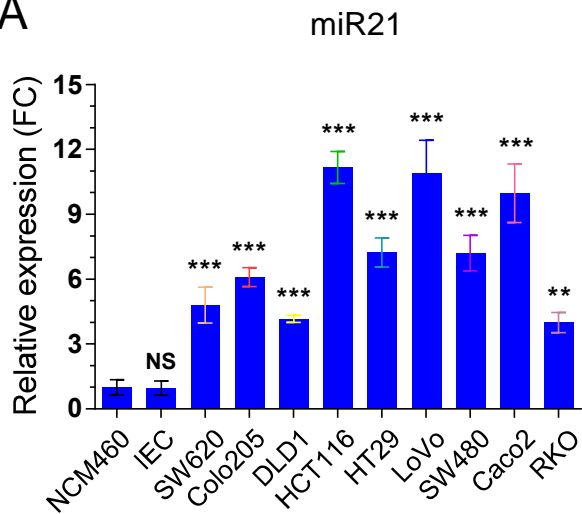
B

LoVo

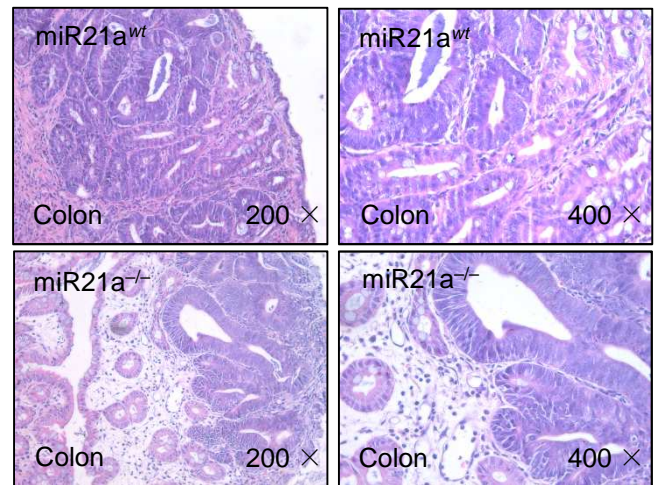


Supplementary Figure 7

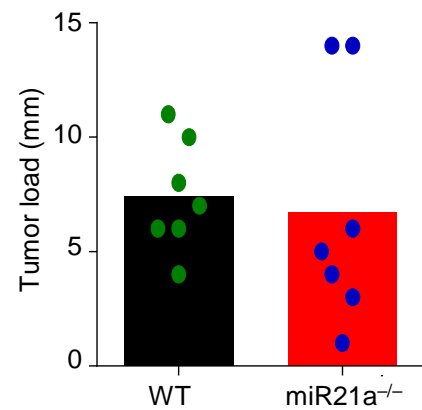
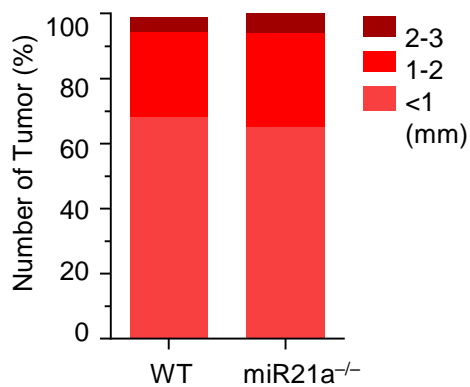
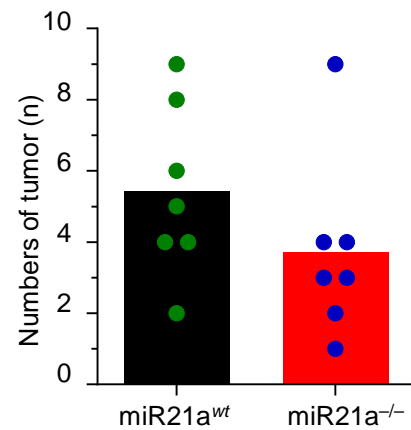
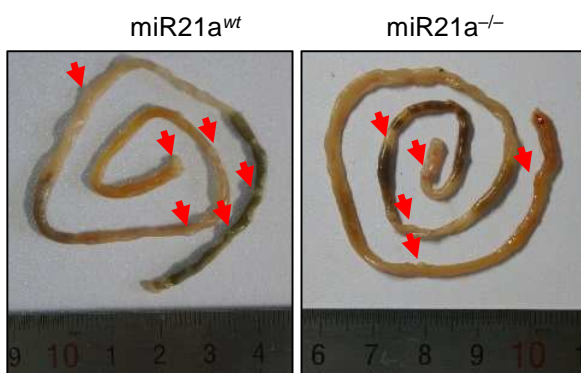
A



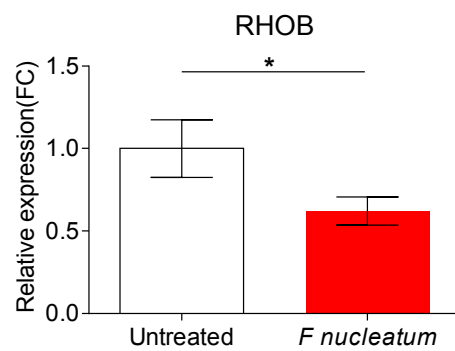
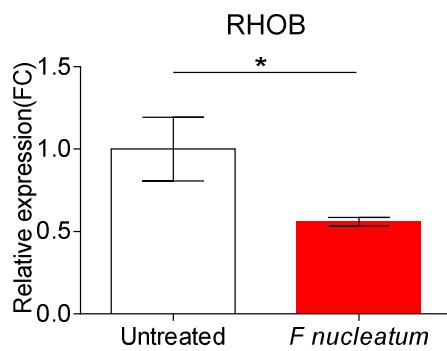
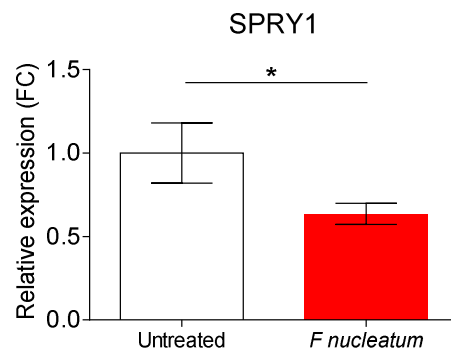
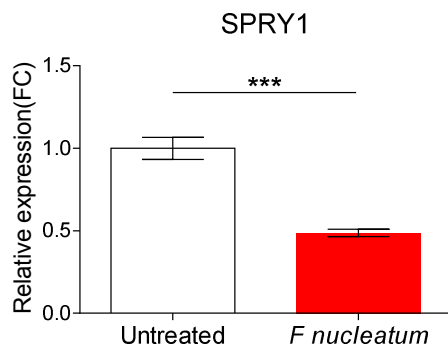
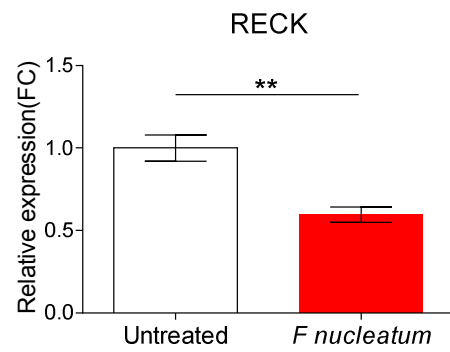
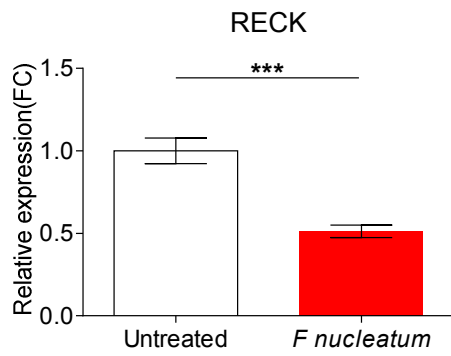
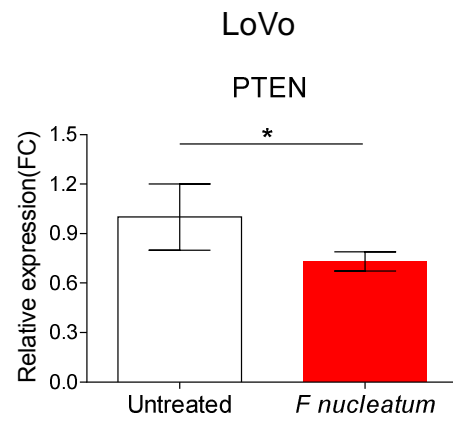
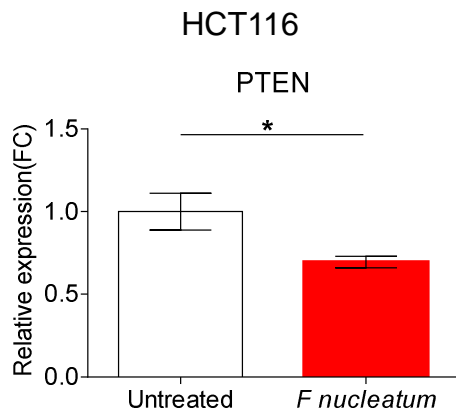
B



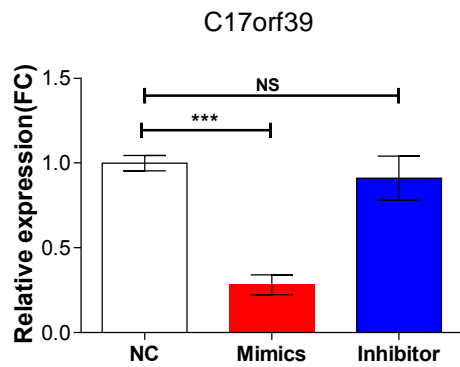
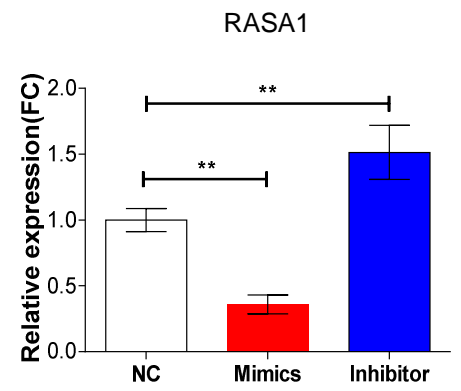
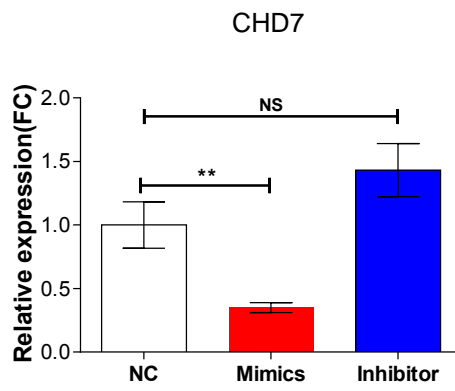
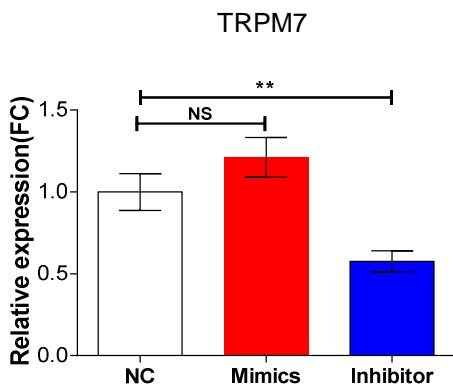
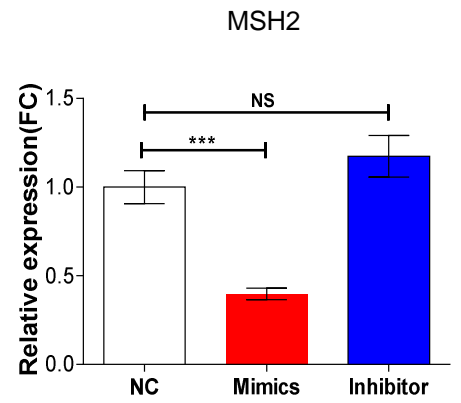
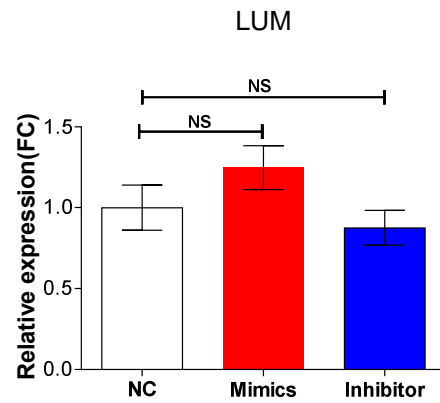
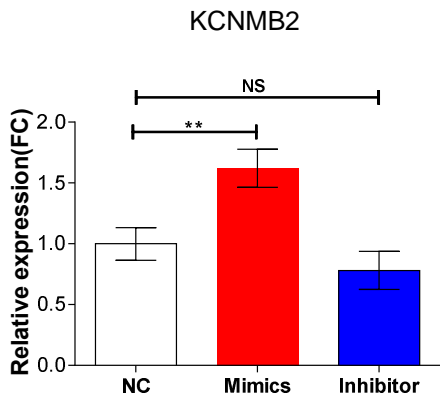
C



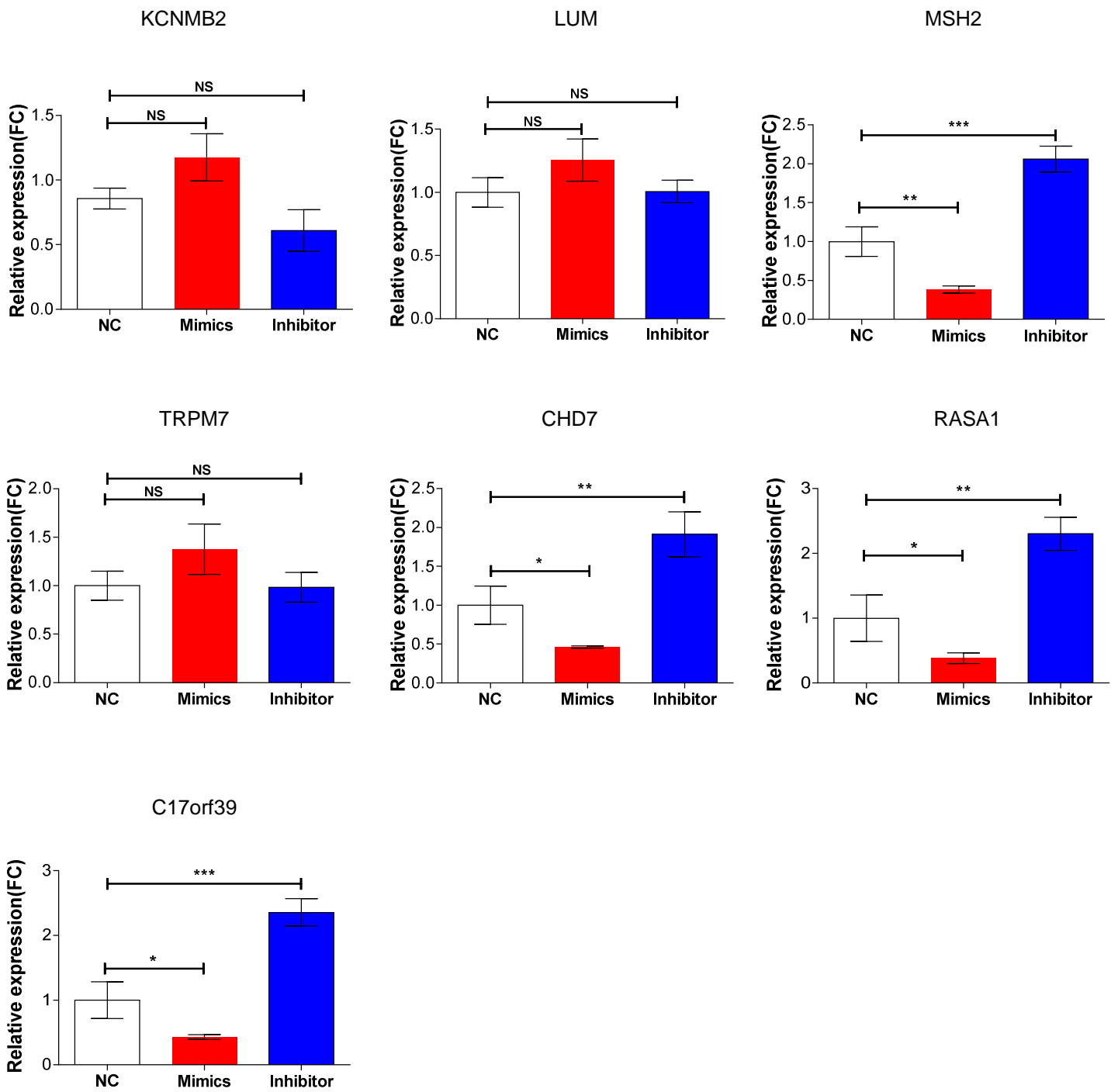
Supplementary Figure 8



Supplementary Figure 9



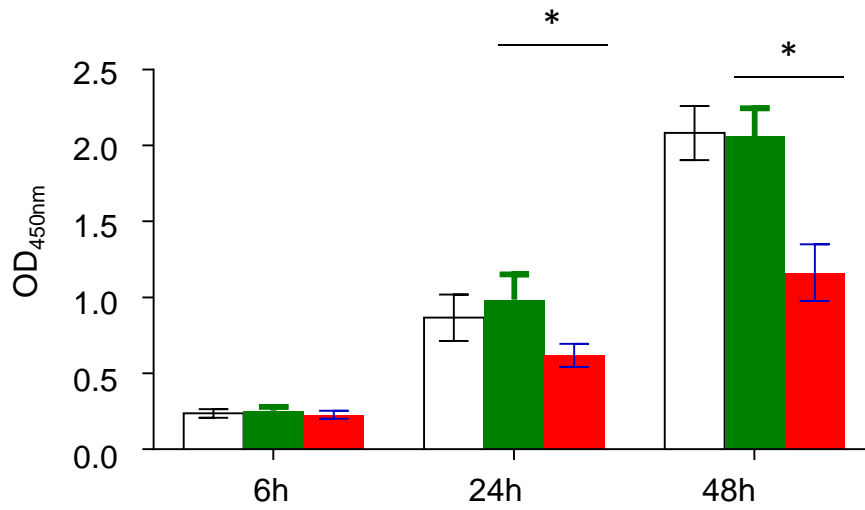
Supplementary Figure 10



Supplementary Figure 11

A

Legend:
□ *F nucleatum*
■ *F nucleatum*/Lv-NC
■ *F nucleatum*/Lv-NFκB



B

